Galaxy Tracers and Velocity Bias

F J Summers[1] and Marc Davis[2]

Astronomy Department, University of California, Berkeley, CA 94720

and

August E. Evrard[3]

Physics Department, University of Michigan, Ann Arbor, MI 48103

ABSTRACT

This paper examines several methods of tracing galaxies in N-body simulations and the effects of these methods on the derived galaxy statistics. Special attention is paid to the phenomenon of velocity bias, the idea that the velocities of galaxies may be systematically different from that of the mass distribution. Using two simulations with identical initial conditions, one following a single dark matter particle fluid and the other following two particle fluids of dark matter and baryons, both collisionless and collisional methods of tracing galaxies are compared to one another and against a set of idealized criteria. None of the collisionless methods proves satisfactory, including an elaborate scheme developed here to circumvent previously known problems. The main problem is that galactic overdensities are both secularly and impulsively disrupted while orbiting in cluster potentials. With dissipation, the baryonic tracers have much higher density contrasts and much smaller cross sections, allowing them to remain distinct within the cluster potential. The question remains whether the incomplete physical model, especially the expected conversion from a collisional gas to a collisionless stellar fluid, introduces systematic biases. Statistical measures determined from simulations can vary significantly based solely on the galaxy tracing method utilized. The two point correlation function differs most on cluster scales (less than 1 Mpc) with generally good agreement on larger scales (except for one systematically biased method). Pairwise velocity dispersions show less uniformity on all scales addressed here. All tracing methods show a velocity bias to varying degrees, but the predictions are not firm: either the tracing method is not robust or the statistical significance has not been demonstrated. Though theoretical arguments suggest that a mild velocity bias should exist, simulation results are not yet conclusive.

Subject headings: cosmology: large-scale structure of universe — galaxies: clustering — galaxies: formation — methods: numerical

N-body simulations of large scale structure have sometimes been referred to as 'experimental cosmology'. Indeed, at the heart of these efforts is the desire to provide stringent tests of various theories of structure development. Much progress has been made in determining which theories produce structure similar to what is observed, but a major obstacle to this progress is the identification of where galaxies would reside in a numerical simulation. Accurate identification of galaxy positions and velocities within the computer models is required in order to provide reliable estimates of important structure measurements such

[1] Present address: Princeton University Observatory, Peyton Hall, Princeton, NJ 08544; summers@astro.princeton.edu

[2] Also Physics Department, University of California at Berkeley; marc@coma.berkeley.edu

[3] evrard@pablo.physics.lsa.umich.edu

as the correlation function and the velocity dispersion of galaxies. Tracing galaxies is also essential for following the processes of galaxy, group, and cluster formation. As the results derived may support or reject a cosmogony, the various methods for tracing galaxies must be evaluated carefully.

During the last decade, particle simulations became a standard tool for evaluating cosmological theories. Simulations were influential in shifting focus away from the hot dark matter scenario (White, Frenk, & Davis 1983) and toward the cold dark matter (CDM) scenario (Davis et al. 1985). Galaxy redshift surveys are routinely compared against computational realizations of cosmological theories in order to assess the viability of the theories (e.g., Efstathiou, Sutherland, & Maddox 1990, Vogeley et al. 1992, Fisher et al. 1995). Simulations have also played a significant role in the recent attention on the mixed dark matter scenario (Davis, Summers, & Schlegel 1992, Klypin et al. 1993). N-body calculations are now an important method for determining the predictions of a cosmological theory in the non-linear regime.

Unfortunately, comparison of a computer model with observations involves several caveats, restrictions, and subtleties of interpretation that limit the range of conclusions that can be made. One of the most important to note is that by no stretch of the imagination does one form 'galaxies' in current cosmological simulations: the physical model and dynamic range are inadequate to follow any but the crudest of details of such complex and rich structures. What one hopes to do is find the likely sites of galaxy formation and trace their evolution. It is the statistics of these galaxy tracers that are used to evaluate the theories and thus, it is of paramount importance that the galaxy tracer population be as reliable as possible.

The importance of the galaxy tracer population has been illustrated quite vividly. In early simulations of the CDM theory, Melott et al. (1983) found that the correlation function of the mass could replicate the observed correlation function of galaxies. Using more detailed simulations and an algorithm for identifying galaxy tracers, Davis et al. (1985) found that galaxies had to be more correlated than the dark matter to get an acceptable fit to the data. The excess correlation strength was termed 'biasing' and their results showed it to be a rather strong effect. Couchman and Carlberg (1992, hereafter CC) also modelled a CDM universe, but, using a different galaxy tracing method, reached a third conclusion. Previously, Carlberg, Couchman, & Thomas (1990) had proposed that the velocity field of galaxies could be systematically lower than that of the dark matter and dubbed this new effect velocity bias in order to differentiate it from the correlation bias. CC found a significant velocity bias such that the data could be consistent with a CDM model where the galaxies were actually slightly less correlated than the dark matter (a mild anti-bias). These claims have sparked a lot of discussion because CDM with large biasing is at odds with several measures of large scale structure such as the APM galaxy distribution (Efstathiou et al. 1990) and the COBE observations (Efstathiou, Bond, & White 1992). From a computational scientist's point of view, one should be very uncomfortable with such a large impact on one's conclusions based heavily on a galaxy tracer algorithm.

Two groups have recently reported a notable improvement in galaxy tracing. The work in our group (Summers 1993, Evrard, Summers, & Davis 1994, hereafter Paper I) will be referred to as SDE and the other group by their author list, KHW (Katz, Hernquist, & Weinberg 1992). The simulations of these researchers employed two particle fluids, one of dark matter and one of baryons (also called gas), and enough physics to follow the collapse of the luminous parts of galaxies directly. For the first time, objects of galactic densities were found in cosmological simulations and reasonable populations of galaxy-like objects could be defined, albeit at considerable computational expense. Interestingly, on the question of velocity bias, SDE found results mostly in accord with CC, while KHW found no evidence for velocity bias.

Some aspects of velocity bias need to be clarified. As Carlberg (1994) points out, there are two forms of velocity bias, one for the global pairwise velocity dispersions, $v_{b,pairwise}$, and one for the velocity dispersions within clusters, $v_{b,cluster}$ (Carlberg refers to these as the two particle and single particle velocity biases, respectively). The first compares the pairwise velocity dispersion of galaxies, or galaxy tracers, to that of the mass distribution. This pairwise velocity bias can be a function of scale and is usually compared at 1 Mpc

$$v_{b,pairwise} = \left.\frac{\sigma_{p,g}}{\sigma_{p,\rho}}\right|_{1\ \mathrm{Mpc}} \tag{1}$$

where σ_p represents a one dimensional pairwise velocity dispersion and the subscripts g and ρ denote the galaxies and the mass, respectively. When considering a single cluster of galaxies, a similar ratio for the cluster velocity bias,

$$v_{b,cluster} = \left.\frac{\sigma_g}{\sigma_\rho}\right|_{\mathrm{within\ cluster}} , \tag{2}$$

indicates the degree to which the galaxy velocities sample the full cluster potential. Carlberg (1994) shows analytically how $v_{b,cluster}$ may be understood, but requires N-body simulations to estimate its value. Because the velocity dispersions in large clusters can dominate the pairwise statistic (Gelb & Bertschinger 1994), the two forms are not independent and may have similar values, a confusing point for researchers. The global statistic, $v_{b,pairwise}$, has been considered by many simulations (Carlberg & Couchman 1989, Carlberg, Couchman, and Thomas 1990, Couchman & Carlberg 1992, Katz et al. 1992, Cen & Ostriker 1992, Evrard et al. 1994) and may be compared to the observed dispersion of galaxies in the nearby universe (Davis & Peebles 1983). The cluster statistic, $v_{b,cluster}$, is important for dynamical estimates of cluster masses and comparison to x-ray observations (Carlberg & Dubinski 1991, Lubin & Bahcall 1993, Katz & White 1994, Carlberg 1994, Frenk et al. 1995).

The current status of velocity bias is somewhat confused, in no small part because making reliable estimates of velocity bias from simulations is quite difficult. One needs a simulation with large enough dynamic range to cover from galaxy scales ($\sim$10 kpc) up to scales that cover a statistically fair sample of the universe ($\sim$100 Mpc). Also, because this

effect may be concentrated in clusters, the ability of the galaxy tracing method to resolve cluster regions is paramount. If dynamical friction is the cause (Carlberg et al. 1990), then the galaxy tracers must be much denser than the surrounding medium in order to test it. Measurements of both forms of velocity bias have ranged from 0.3 to 1.0, but the effect of differing galaxy tracer algorithms is not known. With such a large variation in the conclusions, it is a fair question to ask whether any of the estimates are correct.

This paper evaluates and compares several galaxy tracing methods and examines the results derived from them. Criteria of a what constitutes a 'good' galaxy tracer is developed and applied to the different tracing methods. Using two simulations with the same initial conditions, one with dark matter only and the other employing both dark matter and gas, the various algorithms are considered on an even footing. An understanding of each method's strengths and limitations is required for applying them properly. We also test whether the extra complexity and cost of the two fluid simulations are necessary. In order to get an idea of the consequences when comparing to real data, the correlation and velocity statistics of each population will be examined and contrasted. We will then be able to make better statements on the issue of velocity bias.

1. Criteria and Methods

In order to evaluate the various galaxy tracing methods, it is useful to have a set of ideal criteria that can serve as a basis for judgement. In this respect, the main concern is for finding and following the positions and velocities of the galaxy tracers since these are the basic properties that are used in comparison against real data. Other characteristics such as luminosity, morphology, and internal dynamics provide the details of galaxy formation, but are not strictly necessary for just tracing galaxies. Additionally, the statistical measures of a good tracer population should reflect the assumed cosmology and are not inherent in the tracer algorithms. Thus, finding the expected correlation function does not validate the tracer algorithm. The limitations and ramifications when interpreting these statistics will be discussed in a later section.

The first thing one requires is that the tracers be well defined. The positions and velocities should be uniquely specified and the dependence on the parameters of the algorithm should be weak. Some classification of the galaxy tracers, usually according to mass, is required for one to be able to compare an observed galaxy population against the correct counterpart in the simulation. Often these comparisons will involve further assumptions, such as a mass to light ratio, but the initial basis for comparison must be an attribute of the tracers. These are minimum criteria for an identifiable population.

Further, because one is ostensibly studying galaxies, other criteria are needed. The evolution of an individual tracer should be coherent in that it can be easily tracked from one simulation output to the next. The merging of tracers as well as the possible disruption of a tracer should be addressed by the method. For robust statistical measures, the tracers must be identifiable in both field and cluster environments. And finally, there is a

subjective measure of the plausibility of the tracer selection algorithm for picking out and tracking the likely sites of galaxy formation. Although a plausibility criterion sounds open ended, the emphasis is that the identification and evolution of galaxy tracers be shown to follow a reasonable path and that neither becomes corrupted by numerical artifacts. Satisfying these criteria will not ensure a correct population, but will go a long way toward enhancing one's confidence in the selection method. In most cases, these criteria are useful in identifying the limitations of a population.

The best way to compare the various galaxy tracing methods is to apply each of them to the same simulation. Each method will examine the same particle configurations and will determine what structures it can find. To explore both collisionless and dissipational methods of tracing galaxies, we will use two simulations evolved with the P3MSPH code (Summers 1993, Evrard 1988) from the same initial conditions; the first uses a single collisionless dark matter fluid and the second follows two fluids: dark matter and a dissipational baryonic component. The Two Fluid run was described in detail in Paper I and the DM run is the single fluid version. Important parameters of the simulations include a comoving cubical size of 16 Mpc along a side, a particle count of 262,144 particles per species, and an effective resolution of $\sim 20/(1+z)\,$kpc. The initial conditions use a CDM power spectrum and are constrained to produce a mass concentration characteristic of a poor cluster of galaxies in the center of the region. The DM run has a timestep of 4.3 Myr and a particle mass of $1.08 \times 10^9\,\mathrm{M}_\odot$. The Two Fluid run uses a timestep of 6.1 Myr, has particle masses of $9.72 \times 10^8\,\mathrm{M}_\odot$ and 1.08×10^8 for the dark matter and baryonic particles, respectively, and models thermal pressure, shock heating, and radiative cooling via smoothed particle hydrodynamics (SPH) for the baryonic species. The simulations have sufficient time, length, and mass resolution to follow galaxy formation and can address both field and cluster regions.

Figure 1 shows the major structures to be examined in the simulation at the final time. The left plot shows the dark matter in the entire computational volume and the right plot details the central region, one tenth of the box length on a side. For clarity, the full box plot shows only one fourth of the particles in the simulation. The simulation forms a poor cluster, $3.5 \times 10^{13}\,\mathrm{M}_\odot$, in the center, a group of galaxies above and right of center, and a variety of filamentary structure typical of hierarchical simulations. The central region is dominated by a massive halo with little apparent substructure in the dark matter. This figure will be used as a reference for the tracer algorithms.

2. Collisionless Algorithms

In cosmological theories where the universe is dominated by weakly interacting dark matter, simulations which use a single species of collisionless particles interacting only via gravity are appropriate and offer several advantages. Since gravity is the dominant force on large scales, the galaxy distribution should, for the most part, trace the dark matter distribution. Implementing gravitational physics in simulations is well studied and

the codes are robust and optimized. The caveat is that one cannot state for certain that the baryons in the universe will closely follow the dark matter and one knows that gas physics plays an important role in galaxy formation. Hence, a large amount of leeway is provided by schemes which bias the galaxy distribution relative to the dark matter and the constraints one can place on cosmological models are not as stringent as may have been hoped. Still, the large majority of cosmological simulations are collisionless ones.

We will discuss four collisionless galaxy tracing algorithms. The first two, which we refer to as halos and peaks, are well known in the literature and our discussion will be brief. The third is somewhat newer, having been suggested by Couchman and Carlberg (1992), but was not tested in great detail. The fourth is a new algorithm developed here.

2.1. *Halos*

The most natural method for choosing where galaxies are likely to form is to examine the evolved density field. One identifies dense regions in the dark matter distribution as the dark matter halos of galaxies and of clusters of galaxies. This method is both simple and straightforward.

In practice, one utilizes a grouping algorithm to identify groups of particles as galaxy halos. We will use the friends of friends algorithm (FOF) which gathers into a group all particles separated by less than a specified linking length, η. In the usual custom, the linking length is specified in units of the mean interparticle separation, taken to be L/N for a cube of side length L containing N^3 particles. It is usually more informative to give an overdensity constraint for the groups. We shall quote a value δ_{min} that specifies the minimum overdensity contour of a group and is defined by two particles within a sphere of linking length radius:

$$\delta_{min} = \frac{2\Omega_{sim}}{\frac{4}{3}\pi\eta^3} \tag{3}$$

where this formula applies for equal mass particles and the Ω_{sim} factor represents the overdensity of our simulation volume compared to the background universe (due to constrained initial conditions). Be aware that other researchers may have used a different estimate of the overdensity, namely Ω_{sim}/η^3 (e.g., Davis et al. 1985). Additionally, δ_{min} is the minimum contour level and the averaged overdensity of the group is generally many times larger. The other parameter that needs to be specified is the minimum number of particles required to make a group, N_{min}.

The main problem with the halos method has been recognized from the start (Davis et al. 1985). Simply put, when galaxy sized halos merge to form a cluster, the substructure in the cluster halo is erased in about a crossing time and one cannot continue to track individual galaxy halos within the cluster halo. In terms of the criteria outlined above, the method fails to resolve both field and cluster regions.

An example of the method is shown in Figure 2. We have applied the FOF algorithm to the simulation with $\delta_{min} = 300$, $N_{min} = 30$ and plot the halos in the same views as

shown in Figure 1. The method does a good job in regions where a single dark matter halo can be assumed to contain only one galaxy, but fails to find substructure in the central cluster region where many galaxies would be expected. Figure 3 illustrates the merging process by plotting the particles in the largest halo at an early output and at the end of the simulation. A collisionless fluid quickly erases visual substructure.

2.2. *Peaks*

The peaks method arises naturally from the theory of collapse of density perturbations (Bardeen et al. 1986) and can circumvent most of the merging problems of the halo algorithm. Instead of looking for galaxy tracers in the evolved density field, one examines the initial density field. The procedure, in rough terms, is to smooth the initial density field on a desired filtering scale, to identify peaks in the smoothed field above a given peak height threshold as likely sites for galaxy formation, and to tag a single particle near the center of each peak as a galaxy tracer of that peak. Two versions of the method have been developed: the peak tracer method, when one can resolve galaxy scale peaks (Davis et al. 1985), and the peak/background split, when galaxy scales are not well resolved (White et al. 1987). Park (1991) showed that the results of the two methods are similar.

In terms of the definite criteria described in Section 2, the peaks method satisfies, or can be made to satisfy, all of the concerns. Because one is using a single particle as a tracer of a galaxy, there are no questions about being well defined and coherent. One objection may be that a prescription for merging of the peak tracers must be devised, but it does not raise fatal difficulties (White et al. 1987). Additionally, the method presumes no disruption of galaxies. A particular advantage of this method is that by adjusting the filtering scale and the threshold peak value, one can match the number density of peaks to the number density of the galactic objects being studied at the outset. This should not be considered fine tuning, but rather a requirement that one use the correct simulated population to compare with the population in the data.

The problems of the peaks method lie in its correlation with the evolved density field. Although it is a reasonable expectation, there is no guarantee that galaxies will form only from the highest peaks apparent in the linear density field. Further, phase space mixing and tidal distortions are prominent processes in a collisionless fluid (Moore, Katz, & Lake 1995) and it is not clear that a single particle will accurately trace the evolution of a peak. Katz, Quinn, & Gelb (1993) have addressed the correspondence of linear peak tracers and the evolved density field by comparing the results of the peaks algorithm and the halo algorithm on the same simulation. Their results confirm that both of the above concerns are valid: halos do not necessarily arise from high peaks and high peak particles do not necessarily end up in halos. The high frequency of these occurrences, of order 30%, undermines one's faith in the peaks method. Similar conclusions on the collapse of density peaks were also found by Gelb & Bertschinger (1994) and from a theoretical standpoint by Bertschinger & Jain (1994).

2.3. *Couchman and Carlberg's Method*

Another method for avoiding the merging problems of the halo method was suggested in the CC paper. Their idea was to tag particles in galaxy sized halos before a cluster forms. After the cluster merges, one can use those tagged particles to identify where the galaxies would be inside of the cluster halo. One might think of this procedure as a two stage halo algorithm: identify halos at an early output and then identify groups from those halo particles at a late output. In this manner, one might resolve both cluster and field regions. The idea is a good one, but CC did not adequately show that it works in practice.

The method as described in CC is only a little more complex than the halo method. At a chosen redshift, z_{tag}, one employs a grouping algorithm with parameters δ_{tag} and N_{tag} and tags all particles in those groups. At the final output of the simulation, one performs a grouping operation on only the tagged particles using parameters δ_{fin} and N_{fin}. CC then do a mass range cut of these final groups, accepting only groups with particle numbers between N_{low} and N_{high}. The groups that remain are considered to be galaxy tracers.

There are several problems with this implementation. First, the method allows for only one epoch of galaxy tagging, while the collapse of density peaks is considered to be a continuous process. Galaxy halos must have collapsed by z_{tag} in order to be included in the tracer population. The mass cut applied at the end is ostensibly to select a given mass range of galaxy tracers, but the mass of these tracers is ill defined because the method does not account for infall of material between the time of tagging and the final time. The coherence of the galaxy tracers is also unknown because there is no check that the particles that end up in a final tracer were in proximity to one another at the tagging epoch. And last, although CC state that δ_{tag} and δ_{fin} should ideally be related by corresponding to the same physical density, in practice, they adjust the δ parameters independently.

To explore the CC method in detail, we implemented it, with a couple modifications, on our simulation. Our z_{tag} had to be much earlier than theirs, 6.6 versus 3, because our simulation is focused on forming a cluster of galaxies. At redshift 3, much of the cluster halo had already merged. Similarly, our final output is at $z_{fin} = 1$ instead of at $z_{fin} = 0$, but note that the expansion factor between tagging and final epochs is similar, 3.6 versus 4. With 36 times higher mass resolution, we can implement a constant physical density constraint on δ_{tag} and δ_{fin}. Because we feel it is not well motivated, the mass range cut was not implemented, though we have studied what would happen if it were employed. Since the number of CC tracers found was low compared to the other methods, N_{tag} and N_{fin} were set to 5; what we feel is the minimum number of particles one might justify as a believable group.

The first conclusion is that using constant physical density to define tracers does not work. The natural choice was to set δ_{tag} such as to pick out suitable galaxy halos at the tagging epoch. However, since the average density of the universe falls as R^{-3}, the corresponding δ_{fin} becomes much too restrictive and very few galaxy tracers are found (see Figure 4). The tracers are concentrated in the cluster with very few in the field regions.

Alternatively, if one sets δ_{fin} by what would pick out a good field population at the final time, then δ_{tag} is very low and one tags not only the galaxy halos, but also the filaments and collapsing regions around them. Too many particles are tagged and no structure is found within the final cluster halo (see Figure 5). An intermediate density choice solves neither problem. A constant physical density constraint in this method does not help one resolve both field and cluster regions.

To produce a tracer population from the CC method, it was necessary to choose δ_{tag} and δ_{fin} independently. The results using $\delta_{tag} = 300$ and $\delta_{fin} = 750$ are shown in Figure 6 in the same plots as Figures 1 and 2. As a result of the single tagging epoch, the distribution appears weak in the field regions compared to the halos. There are approximately the same number of halo and CC tracers found in the cluster region and the size of the largest object is significantly reduced for the CC method. However, upon examining the velocity fields of the smaller CC tracers (5–10 particles) in the cluster region, about half are incoherent and will disperse within a crossing time of the cluster. These tracers appear to be chance aggregations of particles originating in different halos at z_{tag}. Such groupings are more common than one might expect because the average density in the cluster region is well above average and a much smaller fluctuation is required to create an anomalous grouping. If one does not include these tracers, the cluster region will be poorly sampled. Based on these results and the concerns about the basic methodology expressed above, the CC algorithm fails several of the galaxy tracer criteria.

An important point should be mentioned about CC's mass range cut. In our simulation, CC galaxy tracers in the cluster region are dominated by a large main halo surrounded by many much smaller ones. Implementing a maximum particle number cutoff, N_{high}, will remove the largest tracer and leave only a shell of tracers around the central region. One essentially removes the potato and leaves only the potato skin (see Figure 7). Statistics of this population would not be robust. Similar effects could have skewed the results presented by CC.

In a recent paper, Carlberg (1994) has made some modifications to the above method. He increases the minimum number of particles to 10 at both epochs and checks for excessive velocity dispersions in the final tracer groups to exclude unbound objects. The resulting method is a small improvement, but it does not address the concerns about a single tagging epoch or the disruption of the tracers while they orbit through the cluster. Results in these tests would only be slightly improved over the CC method. In any case, his new method is much less sophisticated than the most bound algorithm presented below.

2.4. *The Most Bound Algorithm*

While analyzing the CC method, it became apparent that the basic idea was sound, but that several improvements could be made to the implementation. To this end, we have attempted to create a collisionless galaxy tracer algorithm that would withstand the *a priori* objections to the CC implementation. The basic idea is that one would like to catch each forming galaxy just after initial collapse when correspondence between dark

matter halos and galaxies is relatively unambiguous. Since significant tidal dispersion of the outer regions is expected during collisionless merging, one should tag and follow only the core particles of these nascent galaxies. Merging simulations have shown that particles which are in the cores before merging tend to reside in the core of the resulting object (Barnes 1989). At the final time, one can check which cores have remained intact, merged, or been disrupted. We call this method the most bound algorithm (hereafter MB).

The MB algorithm is rather complex. To allow for continuous collapse of galaxies, we search for galaxy halos at 21 epochs evenly spaced in time throughout the simulation. At each output we perform a friends of friends grouping algorithm using a constant overdensity cutoff, $\delta_{min} = 300$. In addition, we remove from these groups any particles that are gravitationally unbound and apply a minimum particle number cutoff $N_{min} = 30$. What we want to do is tag the $N_{tag} = 30$ most bound particles of each halo that has just collapsed.

To identify the recently formed halos, each FOF group is checked to see if it contains any tagged particles (i.e., has this group's core already been tagged?). If yes, then the group is ignored. If no, then the N_{tag} most bound particles are tagged with the output time and group identification. These groups are collectively referred to as the tagging groups. Checks are made to ensure that a few stray tagged particles do not inhibit the tagging of a newly formed halo.

This procedure repeats at each output and builds up a population of tagging groups, each with N_{tag} particles. Then we identify where every tagged particle is at the end of the simulation and, using only these tagged particles, perform an FOF grouping with the same δ_{min} and $N_{min,fin} = 10$. Gravitationally unbound particles could not be removed at this step because we are only using a subset of the particles for grouping. This step identifies where the core particles are at the end and identifies groups of core particles. These final groups will be referred to as tracer groups.

Unfortunately, our search does not stop there. We must check the coherence of these tracer groups and delete stray particles. For each tracer group, the particle tags are examined to find out which tagging groups are represented. Strays are deleted by removing particles from any tagging group represented by fewer than $f = 1/3$ of the original N_{tag} tagged particles. After stray deletion, the tracer groups are patently coherent in that they contain combinations of $f\,N_{tag} = 10$ or more particles that had been identified at higher redshift as being together in phase space. A plot of the resulting 257 tracer groups is shown in Figure 8.

Using the particle tags, one can probe the merging history. If a tracer group contains particles from more than one tagging group, it is considered to be a merger. A tagging group that is not represented in any of the final tracer groups is considered to have been dispersed. Note that it is also possible for a tagging group to be found in more than one tracer group. We call these split groups.

The choices of parameters given above were influenced by several considerations. The

interval between output times is about 210 Myr, a balance between the number of outputs we obtained from the simulation and the collapse time of a resolvable halo. $N_{min} = N_{tag}$ was set small to increase resolution of the method, but large enough that some of the core particles could be scattered and still leave a believable tracer. δ_{min} corresponds to a nominal overdensity for a perturbation that has just collapsed and virialized, the ones we are interested in tagging. The minimum represented fraction, $N_{min,fin} = fN_{tag}$, was based partly on plausibility (how small a fragment would one believe is a *real* tracer) and partly on empirical experience (smaller fragments showed incoherent velocity patterns). Variations of the parameters produced consistent results, though increasing f by more than 50% begins to undermine the method.

The MB method can be shown to satisfy all the definite criteria outlined above. The identification algorithm is well defined and not too sensitive on parameter choice. The minimum resolvable mass of the procedure is determined by the parameter N_{tag}. Coherence, merging, and disruption are dealt with explicitly. As Figure 8 shows, the field and cluster populations are not unreasonable. However, the indefinite criterion, plausibility, requires further investigation.

The tapestry begins to unravel when one does an accounting of the tagging groups. Over the 21 outputs, 402 groups were tagged. The 257 final tracer groups includes 29 mergers of 2 to 11 tagging groups that account for 60 other tagging groups. 3 tagging groups were split into 2 tracer groups each. Thus, the number of tagging groups not represented in any tracer group, that is, the number of dispersed groups, is 88 or 22% of the number that were tagged. This fraction seems rather large and one naturally wonders what happened to these dispersed groups.

The dispersed groups meet two characteristic fates involving the main central halo. Groups that fall in along radial orbits are strongly heated by interactions with the central potential of the cluster and break up completely. The particles diffuse in phase space such that no identifiable core remains. Because of the formation process of groups and clusters of galaxies in hierarchical models, radial orbits are expected to be quite common (Katz & White 1994, Summers, Evrard, & Davis 1995). Other groups that orbit in the central potential are subjected to many more smaller perturbations. Tidal effects cause these groups to elongated along their orbits until their core is stretched apart. Note that the split groups mentioned above are groups in an earlier stage of being tidally stretched to disruption. Figure 9 provides examples of both these types of dispersed groups.

The questions raised by these dispersed groups appear fatal to the algorithm. One may argue that the strongly dispersed groups would be expected to be parts of mergers and that, as long as a merger core remains, not tracing these groups would not affect the population. In practice, this would have to be done on a case by case basis and would be time consuming. The more serious problem is that galaxy tracers orbiting within a cluster seem destined to slowly diffuse and become tidally stretched. This process is in the nature of the collisionless simulation, and not just due to the most bound algorithm. Hence,

although the most bound algorithm is a significant improvement over the halo and CC methods, one concludes that, in general, collisionless galaxy tracers do not seem feasible if the individual galaxy halo cores do not survive as sub-potentials within the cluster halo.

3. SPH Galaxy Tracers

The two fluid version of the simulation offers a marked advantage for identifying galaxy tracers. By including a baryonic species and the relevant gas dynamical processes, one may follow the collapse process past the halo stage. Since the gas species is allowed to radiatively cool, thermal pressure support is released and the gas collapses to densities characteristic of the densities of real galaxies (Paper I). Interpretation of the results should be much cleaner.

We note that the structures in the two fluid simulation, as defined by the dark matter halos, are nearly identical to those of the single fluid simulation. Differences occur in the centers of halos where the existence of a high density baryonic clump has made the dark matter more concentrated. The details of the structure of the central cluster halo has also been modified, but it will not affect the analysis here. No special caveats are needed in comparing the two simulations.

With very high density contrasts in the baryons, picking out SPH galaxy tracers is relatively straightforward. Briefly, we used the FOF grouping algorithm with δ_{min} corresponding to roughly the observed density of a present day galaxy and N_{min} set to the resolution limit of the SPH method (see Paper I for further details). Numerically, these parameters at the final output are $\delta_{min} = 8.7 \times 10^4$ and $N_{min} = 30$ particles. For consistency, we will refer to these groups of particles as SDE tracers instead of using the term galaxy-like objects as in Paper I.

Plots of the SDE tracer distribution in the format of the above figures is presented in Figure 10. The baryons have collapsed to very high overdensities and the tracers are very compact in the particle plots, even though tens of thousands of points are plotted. In the field regions, there is a good correspondence between halos and SDE tracers. A few less SDE tracers are found than halos because, for systems at the resolution limit, there is a time delay between when the halo forms and when the gas inside it has cooled to the required density. In the central region, the reduced cross section of the baryonic tracers helps them avoid the excessive merging of the halos and the inner few hundred kpc is well populated. Being much like the halos, but resolving the cluster region, these galaxy tracers fit all of the objective criteria of §1.

SDE tracers satisfy basic plausibility criteria as well. The use of a gas species that can self consistently follow the collapse process greatly enhances one's faith. The fact that complex identification schemes are unnecessary is also a comfort. In addition, these tracers are the first which bear a resemblance to real galaxy morphology and clustering (Summers 1993, Paper I). The main argument against this method is that other physical processes, such as star formation and associated feedback or ionizing background radiation,

are not included (see §2.2 of Paper I for a detailed discussion). Unmodelled processes may significantly affect the sites of galaxy formation or the evolution of the tracers. It is fair to say that these concerns deal with evolving the state of the art and are not gross omissions in the method. Future work will no doubt improve the method.

Ours is not the only SPH simulation to find galaxy tracers of this sort. In a similar but lower resolution study, KHW employed essentially the same physics in a different code and also formed very high density contrast objects. Their galaxy tracer identification scheme was slightly different and a bit more lenient than ours. To show the robustness of identifying SPH galaxy tracers in our simulation, we investigated the KHW method as well. Following their prescription, we used the SPH measured gas variables to identify all gas particles at overdensities greater than 1000 and with temperature less than 30,000 K. We then ran the FOF grouping algorithm on those particles with $\delta_{min} = 1000$ and $N_{min} = 8$. Note that KHW used the DENMAX procedure (Bertschinger & Gelb 1991) as their grouping algorithm, but, because of the high density contrasts involved, in only a couple cases would this have produced a significant difference.

The KHW tracer population shows minor discrepancies with the SDE tracer population. The lower overdensity cut allowed more tracer groups and more particles in each tracer group into the population. The initial overdensity filter, however, served to avoid spurious additions. These extra groups and particles were not enough to significantly alter the mass function of the tracers (presented in Figure 11). Figure 11 also illustrates that the choice of $N_{min} = 8$ is too lax for our simulation. The integrated mass function flattens at about 30 particles and indicates the resolution limit. KHW also recognized resolution limitations and performed much of their analysis with $N_{min} = 32$. We shall use $N_{min} = 30$ in section 4 below. Apart from these small issues, both algorithms identified the same population of objects.

4. Statistical Measures and Velocity Bias

In the above sections, we tested the reliability of individual galaxy tracer algorithms. Here, we examine the ramifications on the inferred galaxy statistics under each method. Specifically, we shall look at the classic statistical measures used in cosmology, the correlation function and velocity dispersion of galaxies, under each of the tracing methods. There does not exist a 'correct' answer against which the methods can be judged, but one can show the variations in the statistics derived from the different populations. Additionally, the results presented here are from a simulation of a region too small to produce robust statistics and biased by the constraint of forming a cluster of galaxies at the center. The numbers should not be construed as general predictions of the CDM theory.

Five populations of galaxy tracers will be compared. As defined above, they will be referred to as halos, CC, MB, SDE, and KHW. The parameters of each algorithm have been set such as to define approximately the same tracer population, i.e., those with a mass greater than 30 particle masses. The exception is the CC method where the lower mass

cutoff is well defined at the tagging epoch but is unknown at the final output because mass accretion is not considered. The N_{tag} and N_{fin} parameters of the CC method were set as generously as was prudent in order to produce a larger population. The number of tracers for each method, in the order above, was 239, 108, 257, 215, and 238. The deficit in the CC method presumably reflects the single tagging epoch: galaxy halos which form after z_{tag} do not make it into their population. As we naturally consider the SDE algorithm to be the best of these tracer methods, we will use it as the basis for comparison below, subject to the caveats of the previous paragraph.

The correlation functions of the tracer populations are plotted in Figure 12. As expected, SDE and KHW agree well. The differences below 75 kpc can be attributed to the uncertainty of small number statistics. The curves for both the halos and the MB tracers drop under the SDE curve below 500 kpc. Such a drop in correlation is expected for a method that does not adequately resolve clusters (Gelb & Bertschinger 1994). The excess correlation seen in the CC method at all scales is a further result of the single tagging epoch. Density enhancements that are tagged early are the larger peaks of the density field and will naturally aggregate over time and have large correlations (Kaiser 1984). The perturbations which collapse later and would dilute these correlations are not included in the CC population. The agreement of most methods on the largest scales indicates that collisionless methods are adequate to estimate correlations on scales exceeding the largest collapsed structures in the simulations. Given the diversity of galaxy tracing algorithms, the broad agreement on large scales may seem surprising. However, since the collapse is pressureless for both fluids until a shock is reached, the baryons and dark matter should track each other down to the collapsed scale. Only the SPH methods continue to follow the correlations on clustered scales. These results reflect the transition from gravity dominated to hydrodynamics dominated regimes.

The pairwise velocity dispersions of the tracer populations, shown in Figure 13, do not provide a strong discriminant between the methods. The dominant trend in the figure is that the SDE curve remains flat over a large range of scales while the other methods are generally lower at small scales and higher at large scales. The KHW curve differs only below 100 kpc where the data are noisy. At small scales, one would attribute the SDE dispersion to its ability to resolve the cluster center. The methods are converging to similar dispersions at a few Mpc, but projection of this trend to agreement at larger scales can not be verified without a larger dynamic range simulation.

Also plotted in Figure 13 is the pairwise velocity dispersion of the dark matter particles. One sees immediately that all of the tracer algorithms would predict a pairwise velocity bias from the simulation. At a scale of 1 Mpc the ratio of tracer to dark matter velocity dispersion ranges from 0.67 to 0.85. The SPH methods show the biggest effect and the MB method has the least. Being optimistic, one might note that the variation in estimates is not that large and agrees well with a judiciously chosen sample from the literature. One could attribute the range to varying amounts of friction, dynamical or viscous, and biased evolution in the tracer populations. However, these estimates are ho-

mogenized by using the same data set. When using both different tracer methods and different simulations, the variance will increase strongly.

Further, this paper has shown that the tracer algorithms vary widely in their reliability and one may fairly wonder whether any method has measured a true velocity bias. For the halo algorithm, Gelb & Bertschinger (1994) pointed out that a reduced velocity dispersion is expected when one removes the large velocity dispersions within a cluster by representing them as a single halo. When they broke up the large halos into a plausible galaxy distribution, the entire velocity bias signal vanished. This argument would also apply to the CC and MB algorithms in that they are also underrepresenting the clusters. Further, the MB results show that collisionless overdensities are tidally destroyed in the cluster region. Thus dynamical friction would not be an important effect for any of the collisionless tracer methods because the overdensities don't remain tightly bound (a contrary opinion of Carlberg (1994) will be discussed in §5). As the MB method tracks collisionless objects a bit better within the cluster, it is consistent that it should show the least velocity bias. For the SPH tracer methods, the very high overdensities achieved make them prime targets for dynamical friction. However, one can also argue that the absence of star formation has kept the particles gaseous longer than is reasonable and that ram pressure from the intracluster medium has artificially slowed the galaxy tracers. In Paper I, we noted that the stability of the velocity bias to both mass cuts and redshift of observation (see Figure 26 of Paper I) argues against dynamical friction, ram pressure and other secular effects. Here we mention that another possibility is that a steady state is established, fed at large radii by infall and drained at small radii by mergers. Such an idea is motivated by numerical studies that include algorithms for star formation and which show that ram pressure is an important effect for purely gaseous SPH simulations (Summers 1993, Frenk et al. 1995). For each method of tracing galaxies there exists questions as to whether the velocity bias signal is enhanced or even created by charcteristics of the tracing algorithm.

We conclude that definitive predictions on the existence of velocity bias as a general phenomenon awaits further development of galaxy tracing within simulations. Couchman and Carlberg (1992) based their claims on a poor galaxy tracer algorithm and the statistics of their tracer population are not reliable. Carlberg (1994) utilizes much higher dynamic range, but still uses a similar algorithm that does not solve the basic problems with collisionless tracer methods. The velocity bias described in Paper I may be overstated due to ram pressure effects in the cluster. Our previous result and the lack of velocity bias seen by KHW are from simulated regions that are too small for general statistics. The data presented by Lubin and Bahcall (1993, see their Figure 5) indicate that the velocity bias parameters may show factor of 2–4 variation from cluster to cluster. Lacking wide dynamic range simulations that model all of the relevant physical processes, the existence and magnitude of velocity bias remains an open question.

5. Discussion

This paper has examined many of the most popular methods for tracing galaxies in

cosmological simulations. A brief summary of the results will help us to identify future improvements in the methods. One must also recognize the limitations in using simulations to test theories of structure formation and special attention will be paid to the contentious issue of velocity bias. From this discussion, a clear picture of the current state of affairs should emerge.

5.1. *Summary*

In evaluating the basic methodology, four algorithms which identify galaxy tracers in collisionless simulations were considered. The standard methods of identifying dark matter halos from the evolved density field or marking peaks in the initial density field have previously documented deficiencies: the halo method does not resolve cluster regions well and the initial peak tracers show insufficient correlation with the non-linear structures. The algorithm of Couchman & Carlberg (1992) is well motivated, but ill conceived in that it fails to address coherence, continuous formation, and growth of tracers. The most bound algorithm is developed here to circumvent the above problems, but finds that clusters are still poorly resolved due to heating and tidal disruption of tracers. Diffusion in phase spase of a collisionless fluid may be an insurmountable problem.

The addition of smoothed particle hydrodynamics markedly improves the situation. Dissipation produces very high density contrasts that can be traced directly. Minor differences in the results from the methods of Evrard et al. (1994) and Katz et al. (1992) do not favor either algorithm. Rather, the limitations now arise in the physical model of the simulation code, not in the post-processing tracer identification. The addition of a baryonic species opens up questions about the relative roles of processes like ram pressure, radiative cooling, star formation, and supernova in the collapse of a galactic scale perturbation.

Ultimately, one wants to get robust statistical measures from the galaxy tracer algorithms. In a group comparison of the estimated correlation functions, most methods agree at large scales and the methods that do not adequately resolve the cluster show a decline at small separations. The CC method finds excess correlation strength at all scales due to biasing inherent in the algorithm. SPH methods produce the most consistently behaved estimate, as is true for the velocity dispersions as well. The small scale drop in signal is also present in velocity dispersions, but convergence of opinion occurs only on the largest scale addressed here (few Mpc). This variance in statistical estimates by simply changing the tracer method signals the need for caution and careful interpretation of simulation results.

5.2. *Improvements to Tracer Methods*

In future work on collisionless galaxy tracers, the question of the coherence of halos orbiting in a cluster potential will have to be settled. Carlberg (1994) has suggested that increased dynamic range in mass and length scales will remove the problem of two body heating and allow orbits to be traced internal to the cluster. His estimates do not consider the tidal effects due to the cluster and due to other orbiting halos. Work by Moore et

al. (1995) finds that such tidal effects can become the dominant source of heating and lead to dispersal, depending on the assumed density profile of the halos. As there is not a consensus on the infinite resolution limit of collisionless halo density profiles, all would agree that the dissolution of substructure must be probed further.

Other progress on collisionless methods will involve a shift of paradigm. Instead of utilizing post-processing techniques, one can incorporate galaxy tracing ideas into the simulation code. One idea that has been tried is to use "sticky" particles, i.e., particles which undergo inelastic collisions (Carlberg 1988). This method is a crude way to mimic hydrodynamics, but, in our unpublished tests, does not seem to offer much advantage over SPH simulations in CPU time. Alternatively, one might use massless tracers in a most bound algorithm to follow the evolution of the center of the potential well. Like the peaks method, problems here involve following the merging or disruption of these tracers and dealing with individual particle tidal scattering. Another idea is to introduce 'artificial cooling' into a collisionless simulation by collecting particles in a collapsing region into a more massive superparticle. This method is being studied by van Kampen (1995), however one must be careful to avoid spurious numerical effects due to a large mass ratio between particles in a simulation (Peebles et al. 1989, this caution also applies to SPH simulations, although to a lesser degree because hydrodynamic forces tend to dominate gravity in dense regions). All of these ideas have the highly undesirable feature that one has to re-run the simulation in order to change parameters of the galaxy tracing method.

Collisionless simulations will always lack the hydrodynamic processes that determine much of the evolution of the luminous parts of galaxies. For SPH models, the challenge is to investigate the effects of including further physics. An ionizing background radiation at high redshift may suppress the cooling and delay or prevent galactic collapse. Handling star formation has several associated concerns: keeping the particles gaseous can overstate ram pressure effects, transforming gas particles to a collisionless stellar fluid with limited resolution may resurrect phase space diffusion problems, and modelling of supernova energy feedback can effectively control the galaxy formation rate (Navarro & White 1993). Further issues of tracking metallicity and the related cooling of atomic and molecular species will keep the field busy for quite some time. Another limitation is imposed by the mass resolution required for galaxy sized clouds to cool efficiently. The runs described herein are the largest SPH simulations in this area of research and can trace galaxies well in simulations up to about 25 Mpc. This scale is a bit small for determining global statistics of cosmologies. The route past this block will be to perform ensemble sets of these simulations or to utilize parallel techniques to produce larger simulations. The use of SPH in cosmological simulations is also a relatively new field and testing and refining of the algorithm will continue.

The research avenues are not limited to those discussed above. Eulerian (grid based) hydrodynamic codes have been applied to cosmology, but do not currently have sufficient dynamic range to address galaxy formation in other than a heuristic fashion (Cen & Ostriker 1992). Methods of softened LaGrangian hydrodynamics (Gnedin 1995) and moving

mesh algorithms (Pen 1995) can add about a factor of ten improvement to grid techniques. Much wider range will be achieved by three dimensional adaptive grid methods under development (Neeman 1994). The multi-pronged attack on the problem offers a wide base for success.

5.3. *Interpretation of Tracer Statistics*

These improved simulations will best serve as predictions of cosmological models when analyzed carefully. This paper has shown that the influence of galaxy tracing methods must be recognized and stated explicitly. The range of validity of the derived results should be estimated and, where possible, the comparison of several methods can be quite illuminating. To be specific, the correlations of galaxies seem quite robust down to the virialized scale of clusters while velocities are stable only to a scale a few times larger. It would be desirable to have larger simulations which could confirm that these relationships hold into the linear regime.

In general, the results from computer simulations can be viewed in a manner similar to observational data. One is quite comfortable taking into account such things as point spread functions, sky subtraction, smoothing, and model fitting when processing data, and the same types of ideas apply to numerical work. Both author and reader may need to be more careful in noting these details.

A case in point is the discussion of velocity bias. Estimates in the literature span a factor of 3 in value. Different groups disagree about dependence on separation scale, mass of the galaxy population, and observation epoch. Only recently has the distinction between pairwise velocity bias and cluster velocity bias been explicitly stated. We suggest here that much of this variation is due to different galaxy tracing techniques. Even if all tracer methods produced the exact same estimate of velocity bias, the errors in each estimate due to the inadequacies of the individual methods would still demand substantial error bars. The errors introduced by the tracer algorithm typically have not been stated explicitly.

Robust estimates will be a computational challenge. The galaxy formation process must be followed through three stages: pressureless initial perturbation growth, dissipational gas collapse, and establishment of a collisionless stellar fluid. To cover scales from sub-galactic to a fair sample of the universe requires dynamic ranges of order 10^4 in length and 10^7 in mass. Cosmic variance may require an ensemble of simulations to pin down a value for a particular model. Plus, currently there are several cosmological models from which to choose.

On the theoretical side, the nature of velocity bias has yet to be agreed upon. In the absence of damping on short timescales, the velocities of galaxies must reflect the depth of the potential well, however, it is not necessary that galaxies have the same radial distribution as the mass. Those who believe that galaxies have a biased spatial distribution, must accept the corollary that the velocities will also be biased. One may distinguish between the probable sources, dynamical friction, peak biasing, or natural biasing, by

isolating their effects in controlled tests. Additionally, a point that is often lost in the noise is that velocity bias is not an end in itself, but is most relevant when applied to clusters of galaxies and their mass estimates. A biased spatial and velocity distribution implies that the standard virial mass estimation may not cover the full virial radius and may not reflect the total virial mass of the cluster. The increasing data on mass estimates from velocity dispersions, x-ray temperature profiles, and gravitational lensing will allow one to compare different estimates at the same radii and get some measure of the effect in the real universe. Several methods of estimation are important for helping constrain such unknowns as projection effects and mass profile models. An understanding of velocity bias is an important step in characterizing the dynamical evolution of galaxies.

5.4. *Conclusions*

Cosmological simulations are beginning to be able to do what one wanted them to do a decade ago: provide realistic and detailed predictions of the distribution of galaxies that form in a theory. They are a useful, but quite complex tool. A cautious and studied approach is necessary to gain the confidence of the astronomical community in the results.

Galaxy tracers in numerical models can play a critical role in determining the predictions of a simulation. Though much emphasis has heretofore been placed on the evolution codes, considerable focus must also be put on the analysis procedures. None of the galaxy tracing algorithms examined here is perfect. Each algorithm has constraints that must be identified and the ensuing limitations on the results should be specified. The methods of tracing galaxies need to be examined before being implemented: theoretical plausibility does not guarantee practical utility. The future of this field appears to be a strong one, but it will necessarily proceed slowly and steadily.

The authors wish to thank R. Carlberg, N. Katz, and D. Weinberg for helpful discussions. Support for this work was provided by NSF grant AST-8915633 and NASA grant NAGW-2367. Computing resources provided by the San Diego Supercomputing Center and the Center for Particle Astrophysics are gratefully acknowledged.

References

Bardeen, J. M., Bond, J. R., Kaiser, N., & Szalay, A. S. 1986, ApJ 304, 15

Barnes, J. 1989, Nature 338, 123

Bertschinger, E., & Gelb, J. M. 1991, Comput. Phys. Mar/Apr, 164

Bertschinger, E., & Jain, B. 1994, ApJ 431, 486

Carlberg, R. G. 1988, ApJ 324, 664

Carlberg, R. G. 1994, ApJ 433, 468

Carlberg, R. G., & Couchman, H. M. P. 1989, ApJ 340, 47

Carlberg, R. G., Couchman, H. M. P., & Thomas, P. A. 1990, ApJ 352, L29

Carlberg, R. G., & Dubinski, J. 1991, ApJ 369, 13

Cen, R., & Ostriker, J. 1992, ApJ 399, L113

Couchman, H. M. P., & Carlberg, R. G. 1992, ApJ 389, 453

Davis, M., Efstathiou, G., Frenk, C. S., & White, S. D. M. 1985, ApJ 292, 371

Davis, M., & Peebles, P. J. E. 1983, ApJ 267, 465

Davis, M., Summers, F J, & Schlegel, D. 1992, Nature 359, 393

Efstathiou, G., Bond, J. R., & White, S. D. M. 1992, MNRAS 258, 1p

Efstathiou, G., Sutherland, W. J., & Maddox, S. J. 1990, Nature 348, 705

Evrard, A. E. 1988, MNRAS 235, 911

Evrard, A. E., Summers, F J, & Davis, M. 1994, ApJ 422, 11 (Paper I)

Fisher, K., Strauss, M., & Davis, M. 1995, ApJ, submitted

Frenk, C. S., Evrard, A. E., White, S. D. M., & Summers, F J 1995, ApJ, submitted

Gelb, J. M. & Bertschinger, E. 1994, ApJ 436, 491

Gnedin, N. Y. 1995, ApJS, in press

Katz, N., Hernquist, L., & Weinberg, D. H. 1992, ApJ 399, L109

Katz, N., Quinn, T., & Gelb, J. M. 1993, MNRAS 265, 689

Katz, N. & White, S. D. M. 1994, ApJ 412, 455

Kaiser, N. 1984, ApJ 284, L9

Klypin, A., Holtzman, J., Primack, J., & Regös, E. 1993, ApJ 416, 1

Lubin, L. M., & Bahcall, N. A. 1993, ApJ 415, L17

Melott, A. L., Einasto, J., Saar, E., Suisalu, I., Klypin, A. A., & Shandarin, S. F. 1983, Phys. Rev. Lett. 51, 935

Moore, B., Katz, N., & Lake, G. 1995, ApJ, in press

Navarro, J. F., & White, S. D. M. 1993, MNRAS 265, 271

Neeman, H. 1994, private communication

Park, C. 1991, MNRAS 251, 167

Peebles, P. J. E., Melott, A. L., Holmes, M. R., & Jiang, L. R. 1989, ApJ 345, 108

Pen, U. 1995, in preparation
Summers, F J 1993, Ph.D. Thesis, University of California at Berkeley.
Summers, F J, Evrard, A. E., & Davis, M. 1995, in preparation
van Kampen, E. 1995, MNRAS, submitted
Vogeley, M. S., Park, C., Geller, M. J., & Huchra, J. P. 1992, ApJ 391, L5
White, S. D. M., Frenk, C. S., & Davis, M. 1983, ApJ 274, L1
White, S. D. M., Frenk, C. S., Davis, M., & Efstathiou, G. 1987, ApJ 313, 505

Figure Captions

Figure 1 – Two plots which characterize the dark matter distribution in the simulation. Length scales here and throughout are given in physical units at $z = 1$. On the left is the entire simulation volume (a 7 Mpc cube) showing the central group, a second group above and right of center, and various filamentary structures. For clarity, only one fourth of the particles are plotted. The right hand side details the central region, one tenth the box length on a side, and shows all of the particles.

Figure 2 – Two plots of the groups found by the halo algorithm. Format is similar to Figure 1. The left hand plot shows the halos in the entire simulation volume. Note that some halos do not appear distinctly in Figure 1 because only one fourth of the particles are plotted in that figure. The right hand side details the halos in the central region (one tenth the box size) with circles denoting the center of mass positions of the smaller halos. The dominant halo is roughly 400 kpc across and should contain many galaxies.

Figure 3 – An example of the merging of dark matter halos. Both panels are cubic regions three tenths of the box length on a side and show the particles that wind up in the largest halo at the final output. The left hand plot shows the large amount of structure that was evident at $z = 2$ and is erased by the final output, $z = 1$ (shown on the right).

Figure 4 – CC galaxy tracers found when δ_{tag} is used to set a constant physical density criterion. The left panel, at $z_{tag} = 6.6$, shows the particles in the entire box which are tagged by the first grouping algorithm. The right panel, also the entire box, but now at $z_{fin} = 1.0$, shows the particles which pass through the second grouping cut in the CC method and would be classified as galaxy tracers. For clarity, circles have been drawn around the center of mass of the tracers in the right hand panel which lie outside the central region.

Figure 5 – CC galaxy tracers found when δ_{fin} is used to set a constant physical density criterion. Format is the same as Figure 4, except that no circles are drawn in the right hand panel.

Figure 6 – CC galaxy tracers found when setting δ_{tag} and δ_{fin} independently. Format is the same as Figure 2.

Figure 7 – Effects of a mass range cut on the CC tracers in the very central region. These plots show the CC galaxy tracers in a cubic region with side length one twentieth of the box length (350 kpc, one half that of the right plot in Figure 6). The left panel shows the largest tracer, which would be excluded from a tracer population by a mass range cut. The right panel shows the tracers that remain after the largest one is removed from the region.

Figure 8 – Galaxy tracers found with the Most Bound algorithm. Format is the same as Figure 2.

Figure 9 – Tidal interactions on MB galaxy tracers. Shown here are two groups that were tagged by the MB algorithm, but which have become tidally dispersed by the end of the simulation. Both panels show the same 700 kpc cubic region as the right panel of Figure 8, but from different projections. Velocities are relative to the center of mass velocity and are plotted as tails. The left panel gives an example of a tracer that has been tidally extended along its orbit through the central halo. The tracer in the right panel has been scattered throughout the region by interactions with the central potential.

Figure 10 – Galaxy tracers found using the algorithm of SDE. Format of the plots is the same as Figure 2, but the central region is shown in a different projection.

Figure 11 – Integrated mass function of the SDE and KHW galaxy tracers. The number of tracers greater than a given mass is plotted versus mass down to the resolution limit of the methods. Mass here refers to the baryonic mass in the tracers.

Figure 12 – Correlation functions for the galaxy tracing methods discussed in section 4. The comoving length scales are twice the physical scales given in previous figures because the simulation was stopped at $z = 1$.

Figure 13 – Pairwise velocity dispersions of the galaxy tracers for the methods discussed in section 4. Also plotted is the pairwise velocity dispersion of the dark matter particles, i.e., the velocity dispersion of the dominant mass.

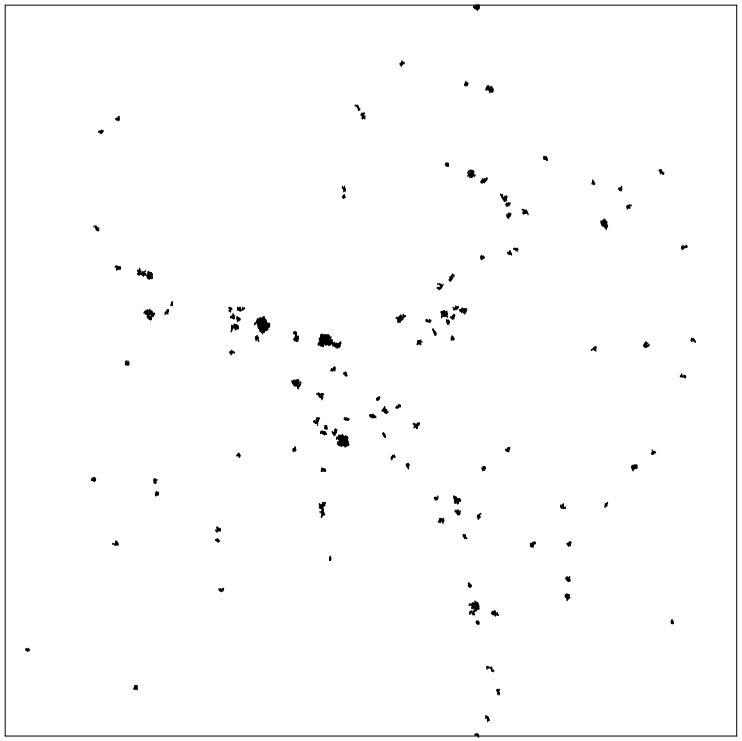

Tagging Epoch – Full Box – 7 Mpc

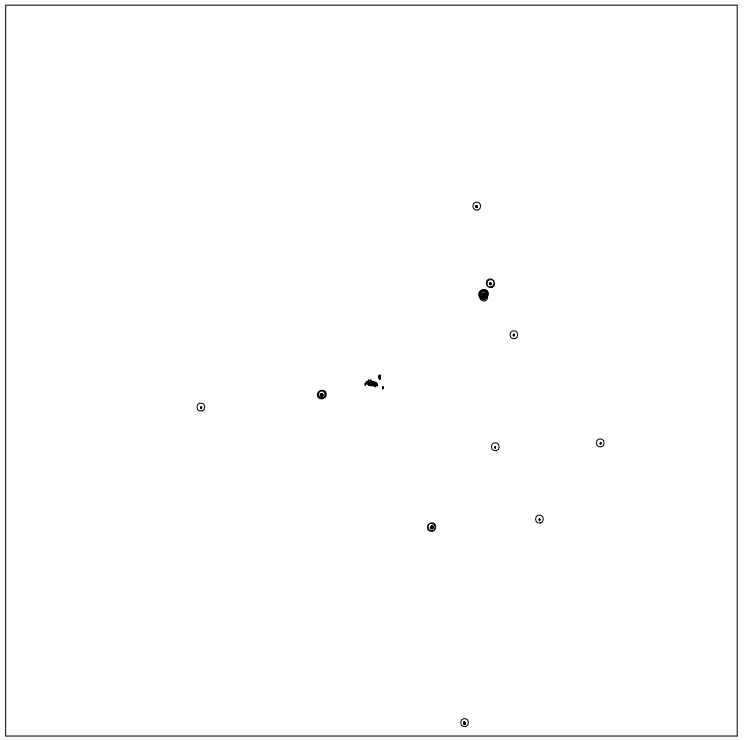

CC Galaxy Tracers – Full Box – 7 Mpc

Figure 4

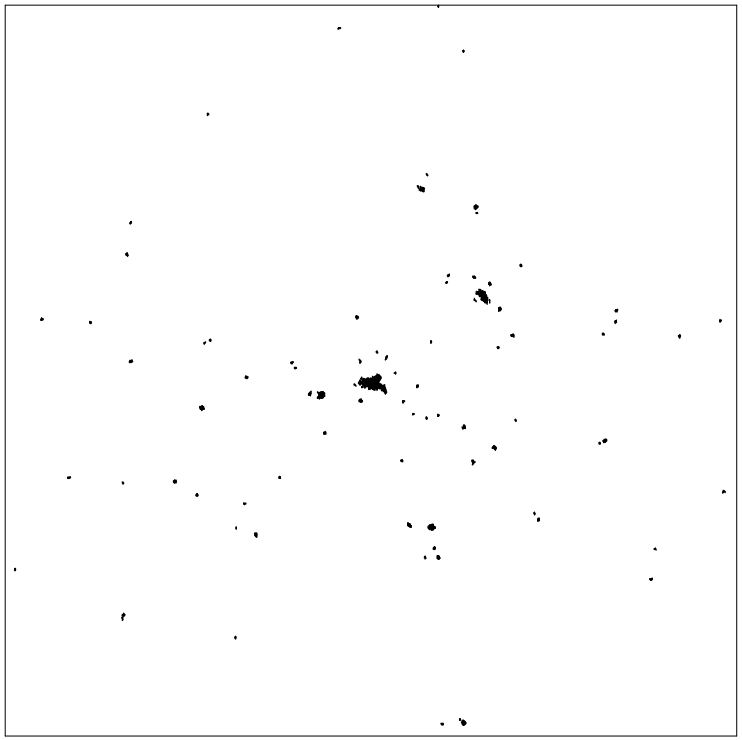

Full Box – 7 Mpc

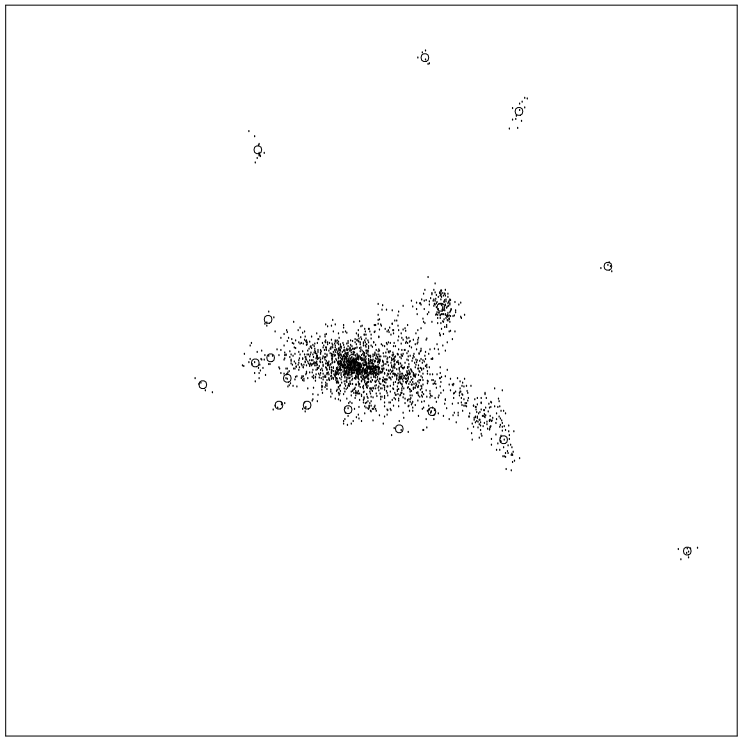

Central Region – 700 kpc

Figure 6

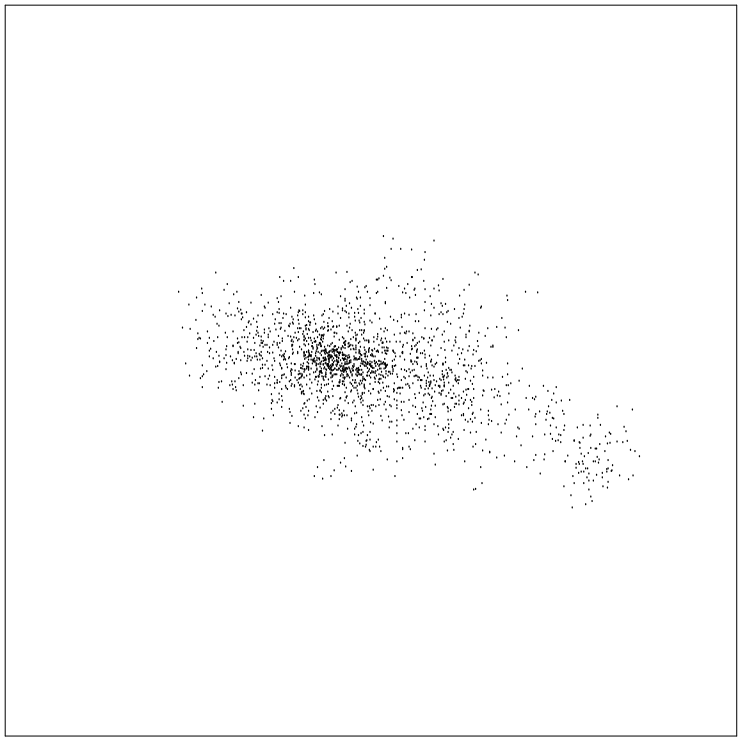

Largest CC Tracer – 350 kpc Region

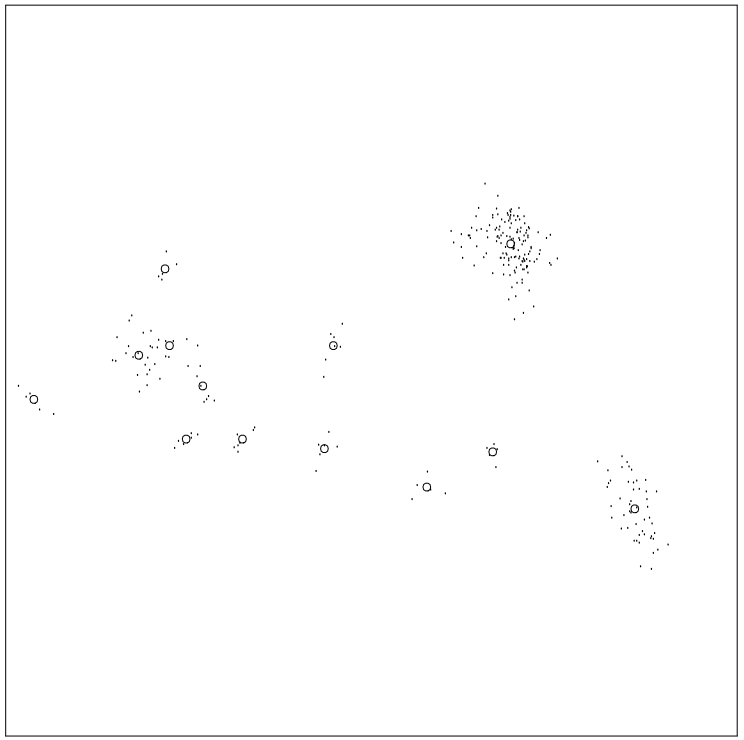

Other CC Tracers – 350 kpc Region

Figure 7

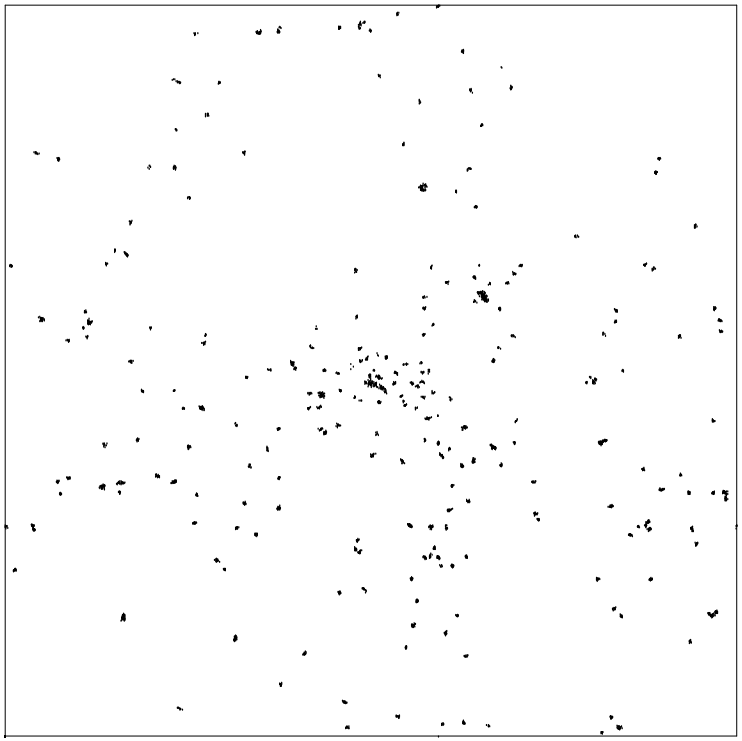

Full Box – 7 Mpc

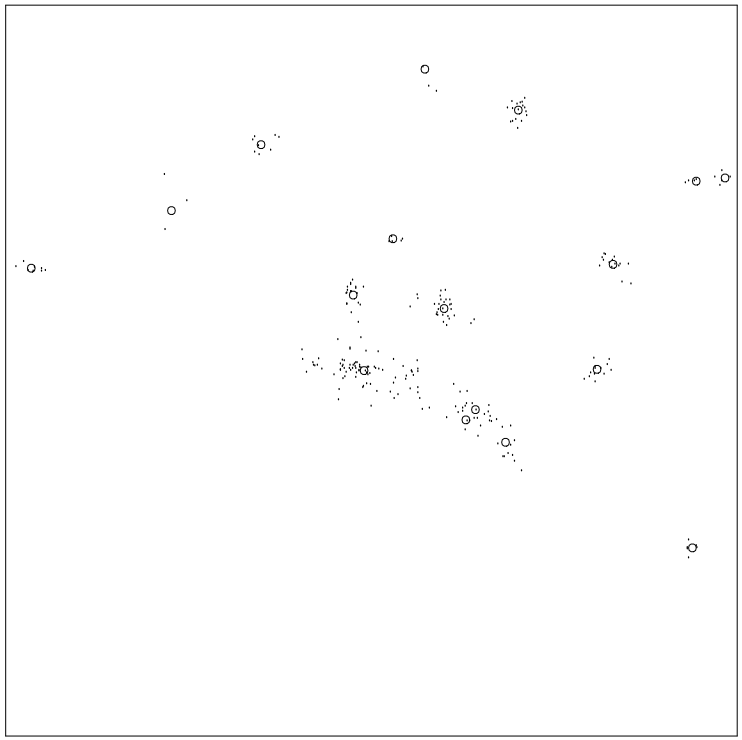

Central Region – 700 kpc

Figure 8

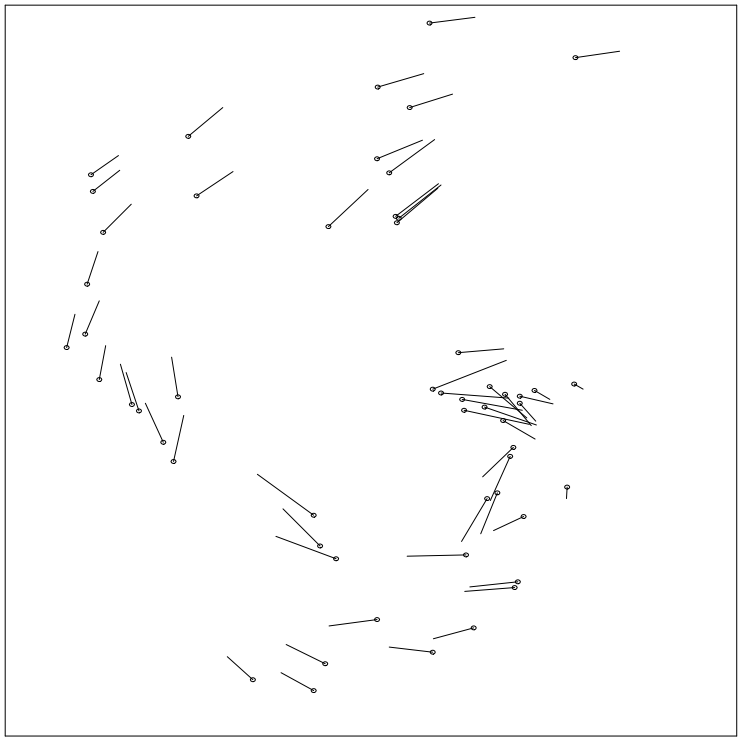

Tidal Stream – 700 kpc Region

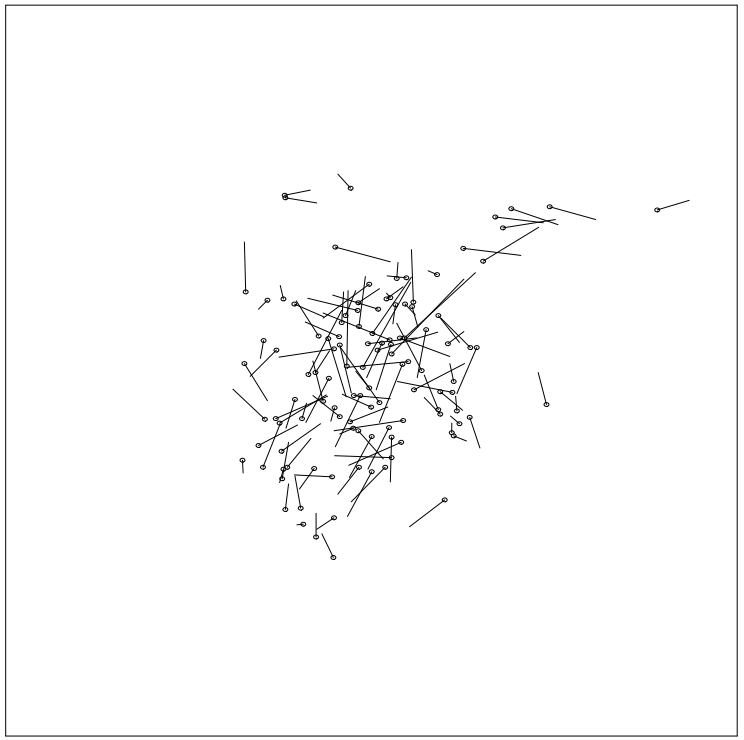

Disrupted – 700 kpc Region

Figure 9

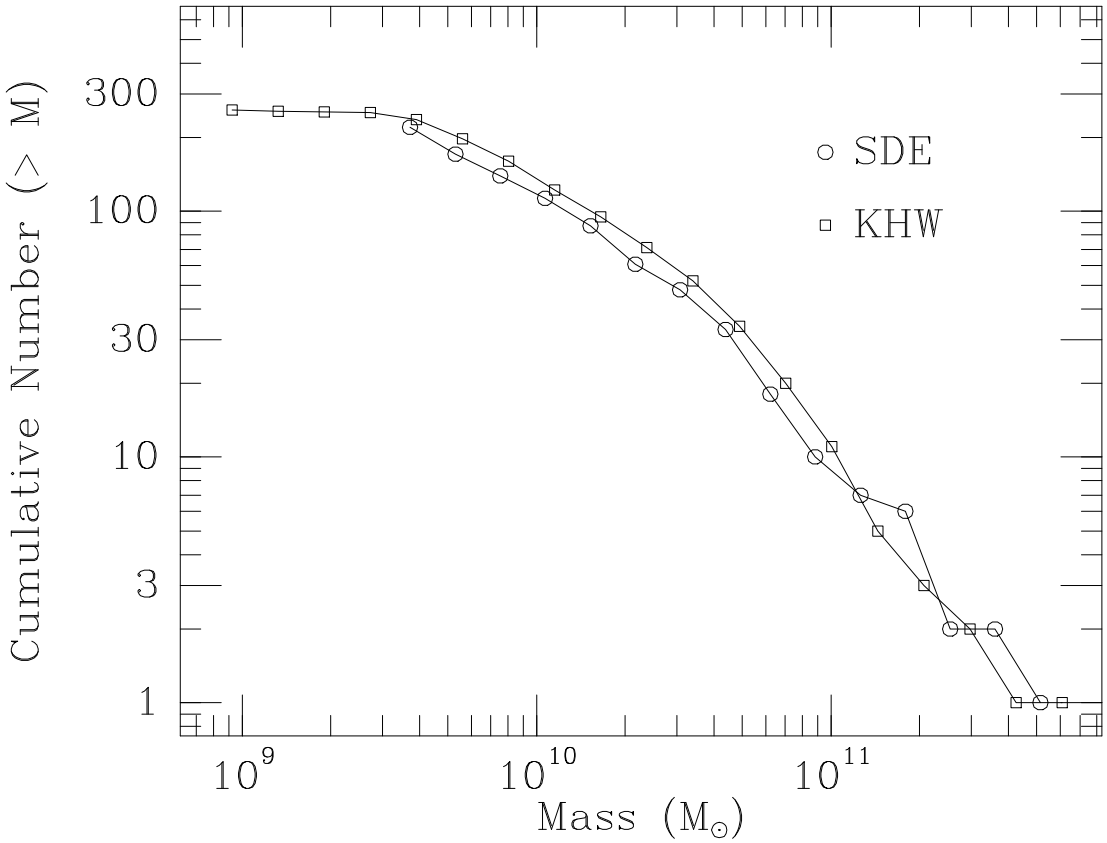
Cumulative Number (> M)
300
100
30
10
3
1
SDE
KHW
10^9
10^{10}
10^{11}
Mass ($M_\odot$)

Figure 11

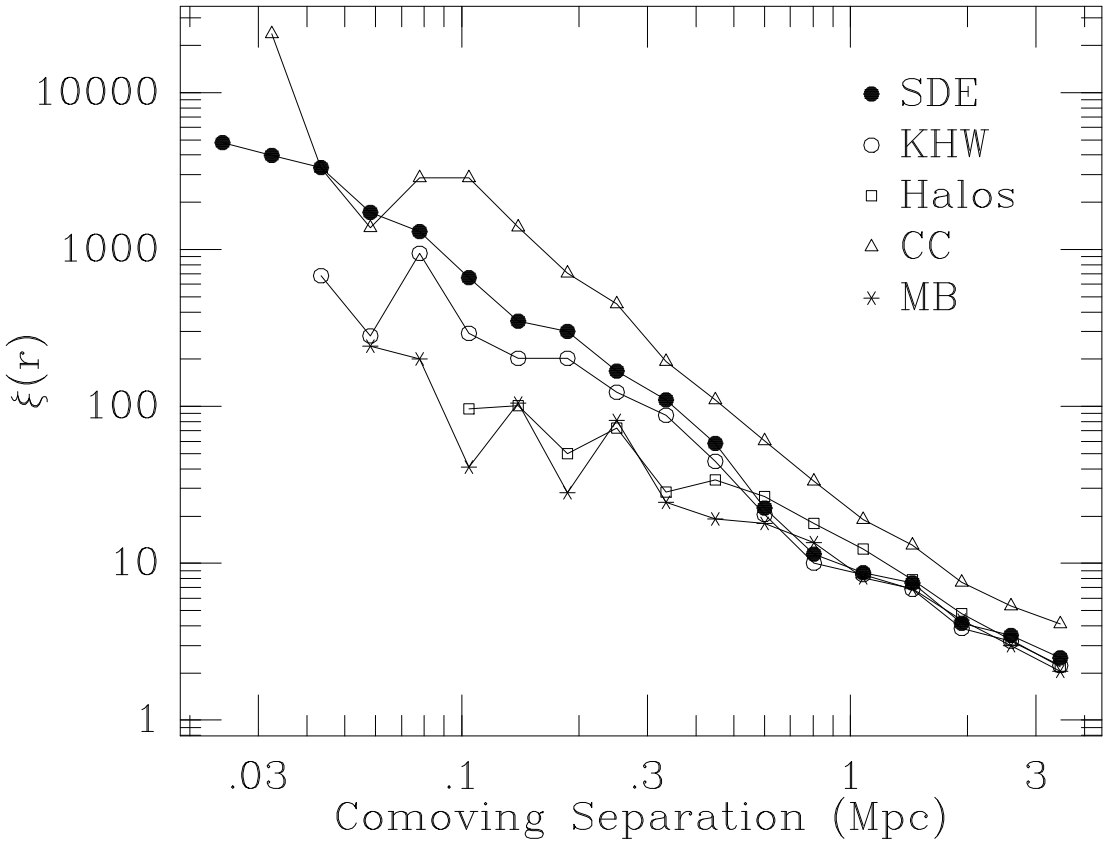
10000
1000
100
10
1
ξ(r)
.03
.1
.3
1
3
Comoving Separation (Mpc)
SDE
KHW
Halos
CC
MB

Figure 12

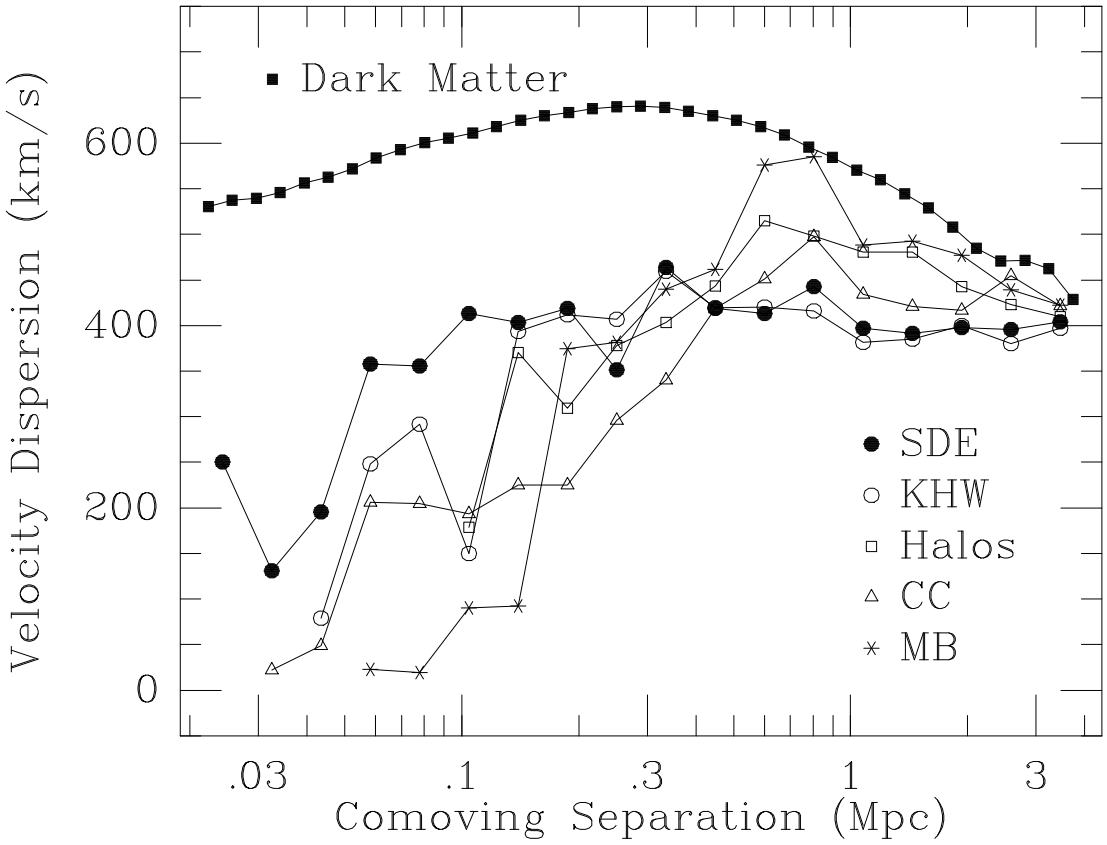
Dark Matter
SDE
KHW
Halos
CC
MB
Velocity Dispersion (km/s)
0
200
400
600
.03
.1
.3
1
3
Comoving Separation (Mpc)

Figure 13